

Supplementary Information for

Highly Efficient Metal-Free Electrocatalysts toward Oxygen Reduction Derived from Carbon Nanotubes@Polypyrrole Core-Shell Hybrids

Hongli An, Ruikang Zhang, Zhenhua Li, Lei Zhou, Mingfei Shao*and Min Wei*

State Key Laboratory of Chemical Resource Engineering, Beijing University of
Chemical Technology, Beijing 100029, China

E-mail: shaomf@mail.buct.edu.cn (M. Shao); weimin@mail.buct.edu.cn (M. Wei)

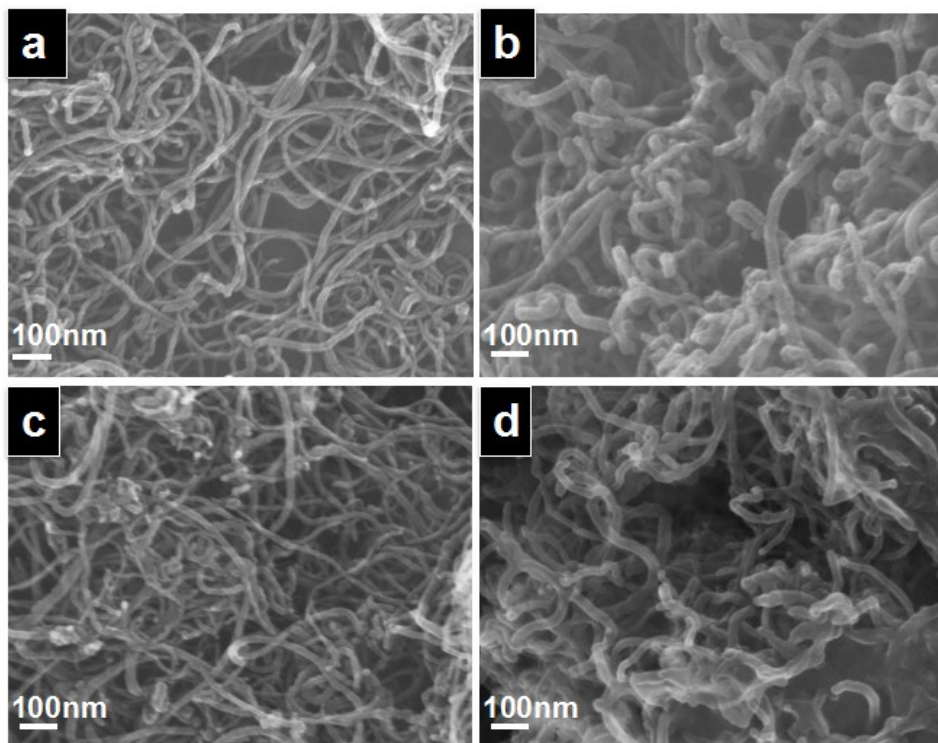


Fig. S1 SEM images of (a) CNTs, (b) CNTs@PPy, (c) CNTs-P800, and (d) CNTs@PPy-P800, respectively.

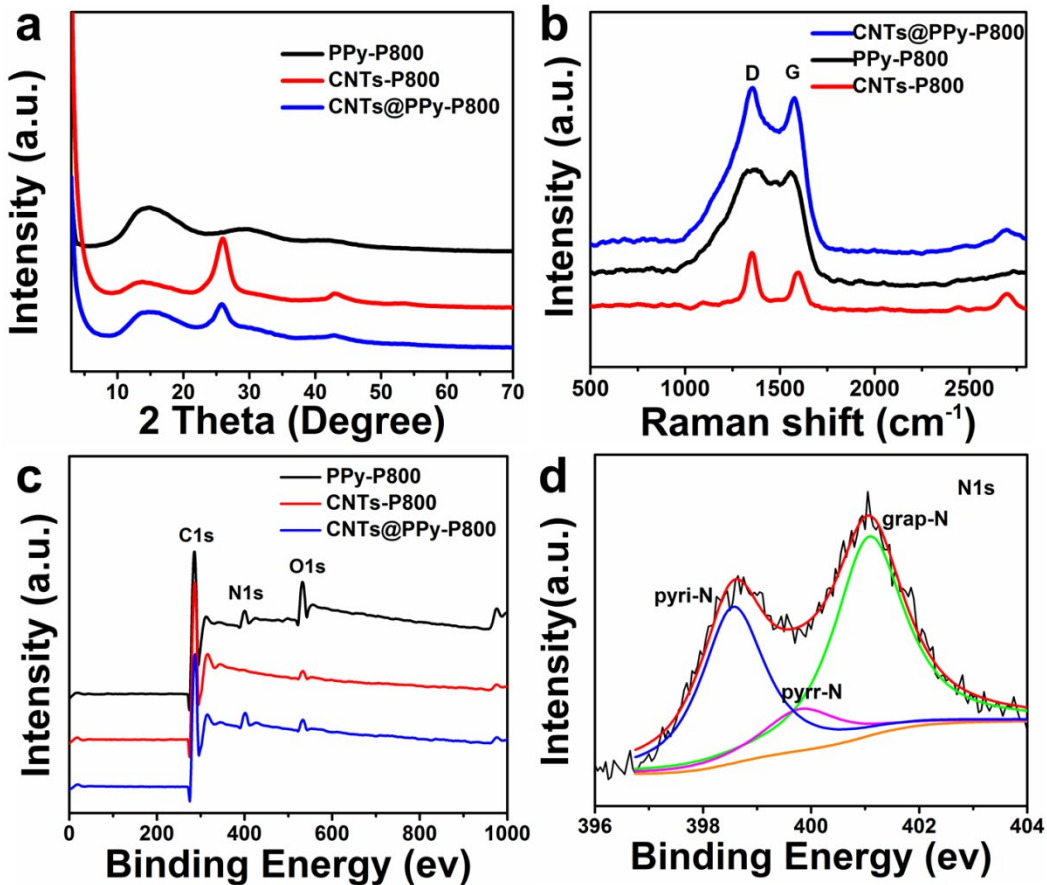


Fig. S2 (a) XRD patterns of PPy-P800, CNTs-P800, and CNTs@PPy-P800. (b) Raman spectra of CNTs-P800, PPy-P800, and CNTs@PPy-P800. (c) XPS survey spectra of PPy-P800, CNTs-P800, and CNTs@PPy-P800. (d) High resolution scans of N1s for CNTs@PPy-P800.

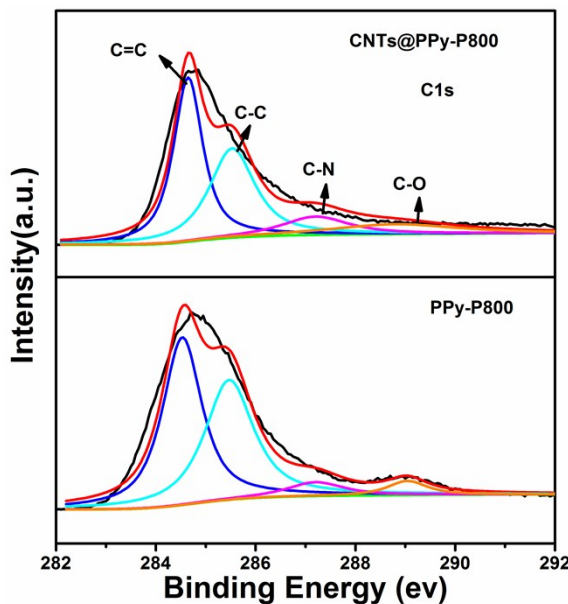


Fig. S3 High resolution scans of C1s for the PPy-P800 and CNTs@PPy-P800.

Table S1. Percentage of various carbon species as a function of PPy-P800 and CNTs@PPy-P800.

Sample	C=C(%)	C-C(%)	C-N(%)	C-O(%)
PPy-P800	48.02	42.33	5.64	4.01
CNTs@PPy-P800	42.61	35.84	10.73	10.82

Table S2. Comparison of the onset potential, half-wave potential and current density for CNTs-P800, PPy-P800, CNTs@PPy-P800, and Pt/C

Sample	E _{onset} vs. RHE (V)	E _{1/2} vs. RHE (V)	Current density (mA cm ⁻² at 0.2V)
CNTs-P800	0.82	0.65	3.36
PPy-P800	0.78	0.58	4.00
CNTs@PPy-P800	0.95	0.81	6.82
Pt/C	0.94	0.80	4.94

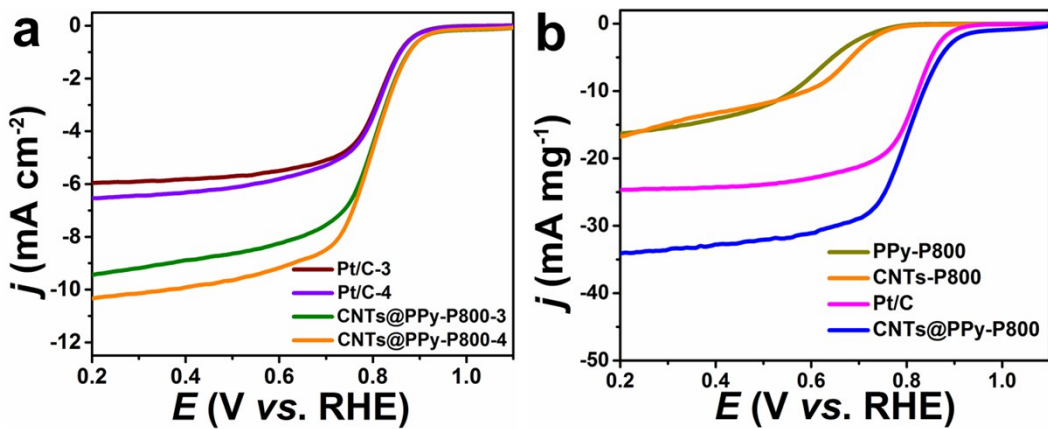


Fig. S4 (a) LSV curves of CNTs@PPy-P800, and Pt/C with different catalyst loading (3 mg cm^{-2} , 4 mg cm^{-2}). (b) LSV curves of PPy-P800, CNTs-P800, CNTs@PPy-P800,

and Pt/C catalyst in O₂-saturated 0.1 M KOH solution at a sweep rate of 10 mV s⁻¹ and electrode rotation speed of 1600 rpm.

Table S3. Current density at 0.2 V for CNTs@PPy-P800 and Pt/C with different catalyst loading (0.2mg cm⁻², 0.3mg cm⁻², 0.4mg cm⁻²)

Sample	0.2mg cm ⁻²	0.3mg cm ⁻²	0.4mg cm ⁻²
Pt/C	4.94 mA cm ⁻²	5.98 mA cm ⁻²	6.54 mA cm ⁻²
CNTs@PPy-P800	6.82 mA cm ⁻²	9.42 mA cm ⁻²	10.32 mA cm ⁻²

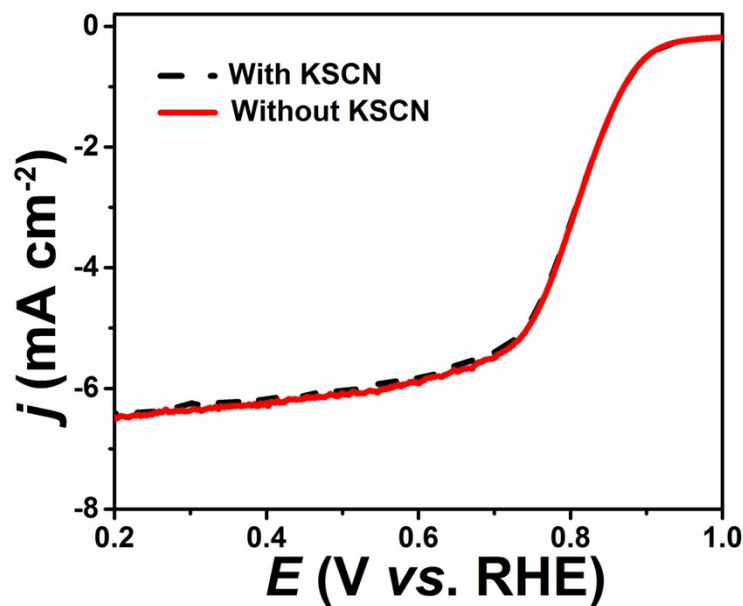


Fig. S5 LSV curves for CNTs@PPy-P800 without and with 10 mM KSCN.

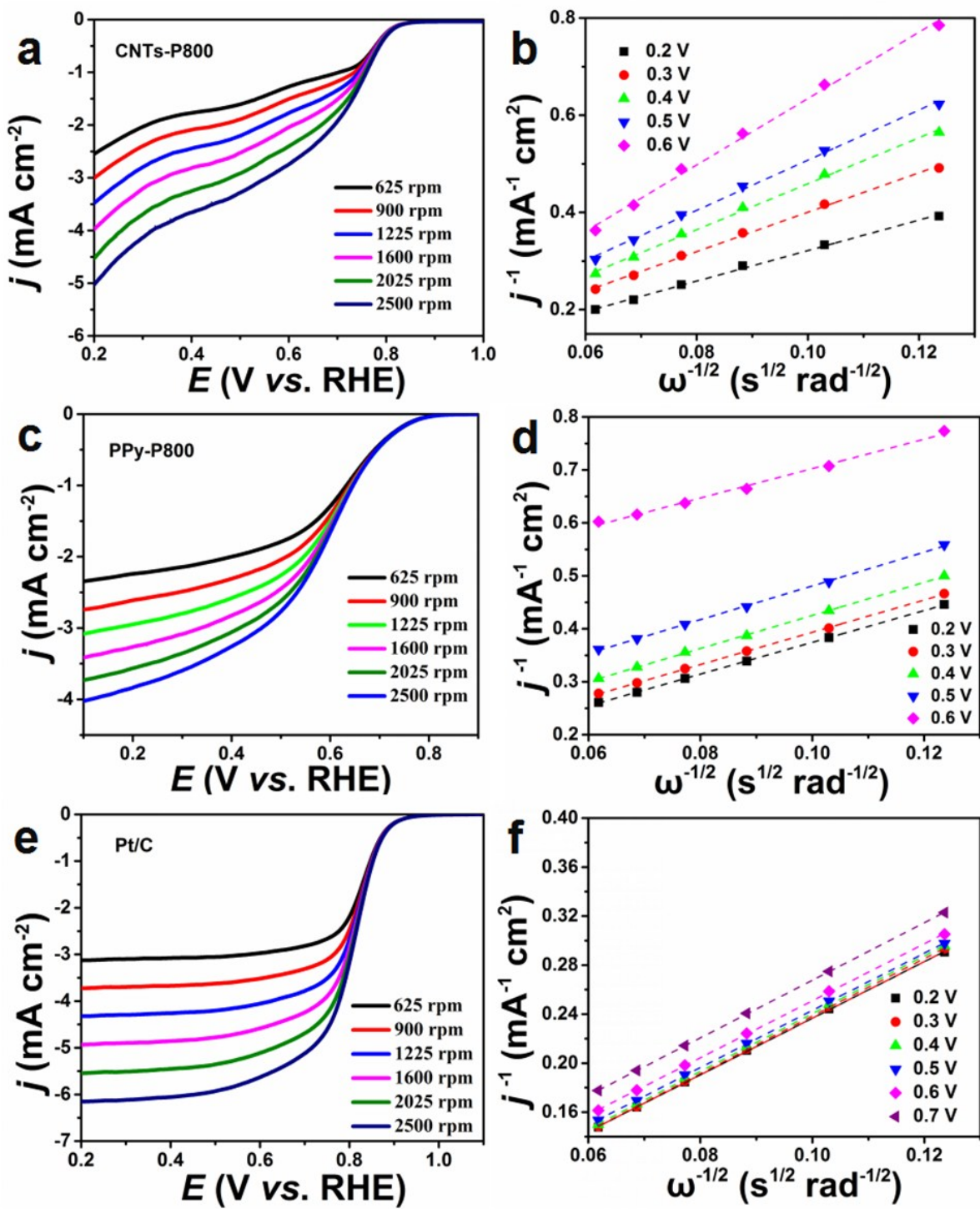


Fig. S6 LSV curves for (a) CNTs-P800, (c) PPy-P800, and (e) Pt/C at the rotation rates of 625 to 2500 rpm, respectively. The corresponding K-L plots derived from the RDE data for (b) CNTs-P800, (d) PPy-P800, and (f) Pt/C, respectively.

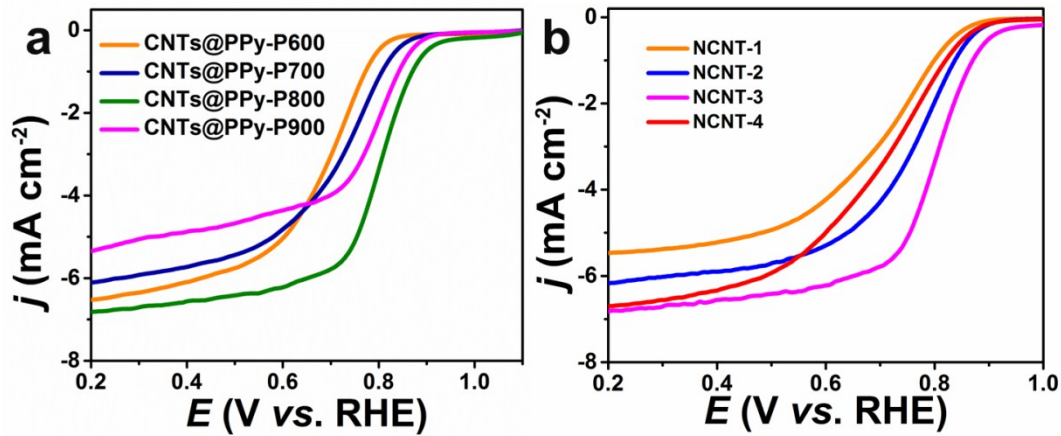


Fig. S7 (a) LSV curves of CNTs@PPy- T ($T = 600, 700, 800, 900$ °C, respectively).

(b) LSV curves of NCNT- x ($x = 1, 2, 3$ and 4 , respectively)

Table S4. Comparison of the onset potential, half-wave potential and current density

for CNTs@PPy- T ($T = 600, 700, 800, 900$ °C, respectively) obtained in this work

Sample	$E_{\text{onset}} \text{ vs.}$ RHE (V)	$E_{1/2} \text{ vs.}$ RHE (V)	Current density (mA cm ⁻² at 0.2V)
CNTs@PPy-P600	0.83	0.69	6.51
CNTs@PPy-P700	0.87	0.72	6.12
CNTs@PPy-P800	0.95	0.81	6.82
CNTs@PPy-P900	0.89	0.77	5.30

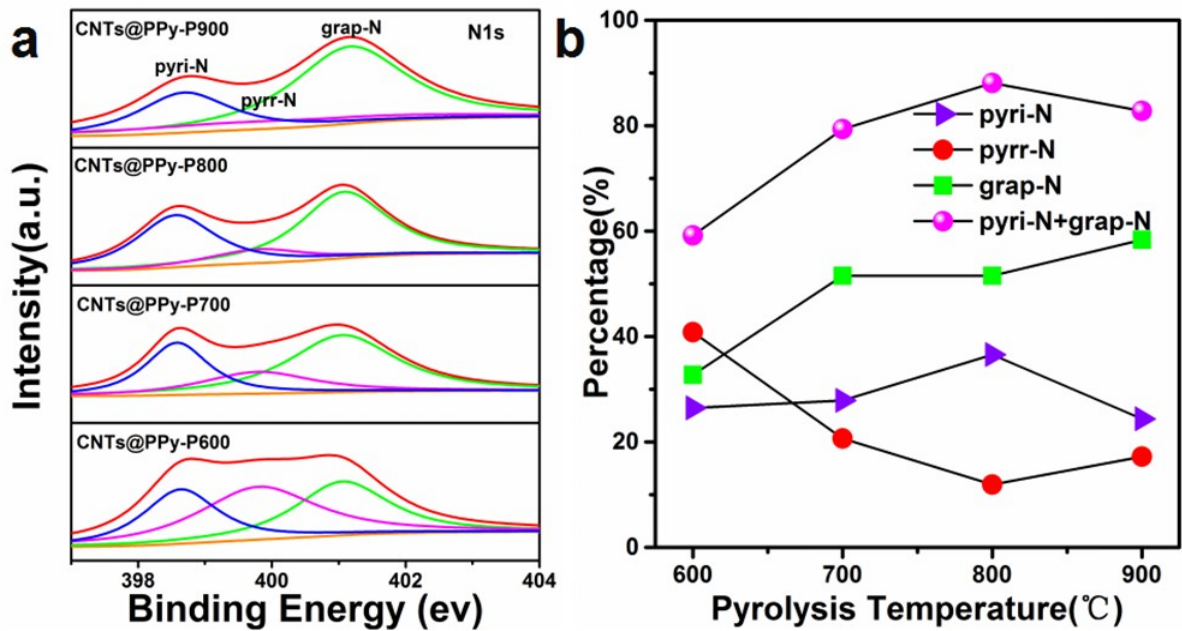


Fig. S8 (a) N1s XPS spectra and (b) Percentage of various nitrogen species of CNTs@PPy- T ($T=600, 700, 800$ and $900\text{ }^{\circ}\text{C}$, respectively).

Table S5. Percentage of various nitrogen species as a function of pyrolysis temperature.

Sample	pyri-N/ N_{total} (%)	pyrr-N/ N_{total} (%)	graphitic-N/ N_{total} (%)	(pyri-N+graphitic-N)/ N_{total} (%)
CNTs@PPy-P600	26.45	40.8	32.75	59.2
CNTs@PPy-P700	27.85	20.64	51.51	79.36
CNTs@PPy-P800	36.58	11.89	51.53	88.11
CNTs@PPy-P900	24.39	17.24	58.37	82.76

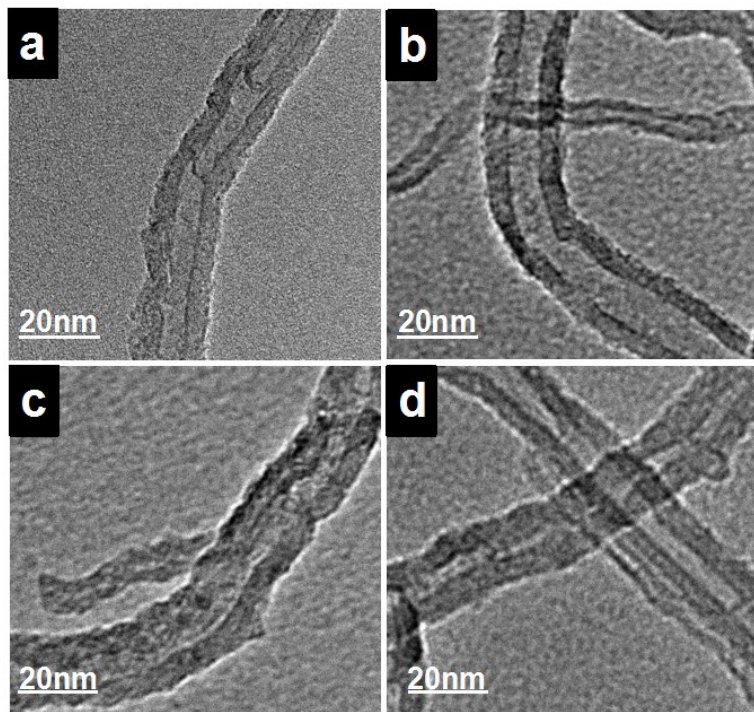


Fig. S9 HRTEM images of (a) NCNT-1, (b) NCNT-2, (c) NCNT-3, and (d) NCNT-4.

Table S6. Comparison of the onset potential, half-wave potential and current density for NCNT-x ($x = 1, 2, 3$ and 4 , respectively)

Sample	$E_{\text{onset}} \text{ vs. RHE (V)}$	$E_{1/2} \text{ vs. RHE (V)}$	Current density (mA cm^{-2} at 0.2V)
NCNT-1	0.87	0.71	5.5
NCNT-2	0.90	0.78	6.2
NCNT-3	0.95	0.81	6.82
NCNT-4	0.9	0.73	7.25

Table S7. The elements content of NCNT-x ($x = 1, 2, 3$ and 4 , respectively)

Sample	C(%)	O(%)	N(%)
NCNT-1	93.08	4.86	2.06

NCNT-2	91.00	3.65	5.35
NCNT-3	88.50	4.59	6.90
NCNT-4	88.14	3.97	7.89

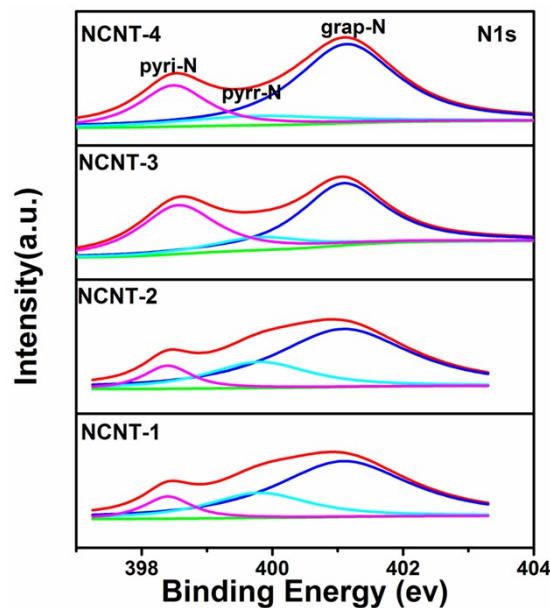


Fig. S10 (a) N1s XPS spectra of NCNT-x ($x = 1, 2, 3$ and 4 , respectively).

Table S8. Percentage of various nitrogen species of NCNT-x ($x = 1, 2, 3$ and 4 , respectively)

Sample	pyri-N/ N_{total} (%)	pyrr-N/ N_{total} (%)	graph-N/ N_{total} (%)	(pyri-N+graph-N)/ N_{total} (%)
NCNT-1	9.68	22.85	67.47	77.15
NCNT-2	12.15	21.92	65.93	78.08
NCNT-3	36.58	11.89	51.53	88.11
NCNT-4	22.92	11.9	65.17	88.10

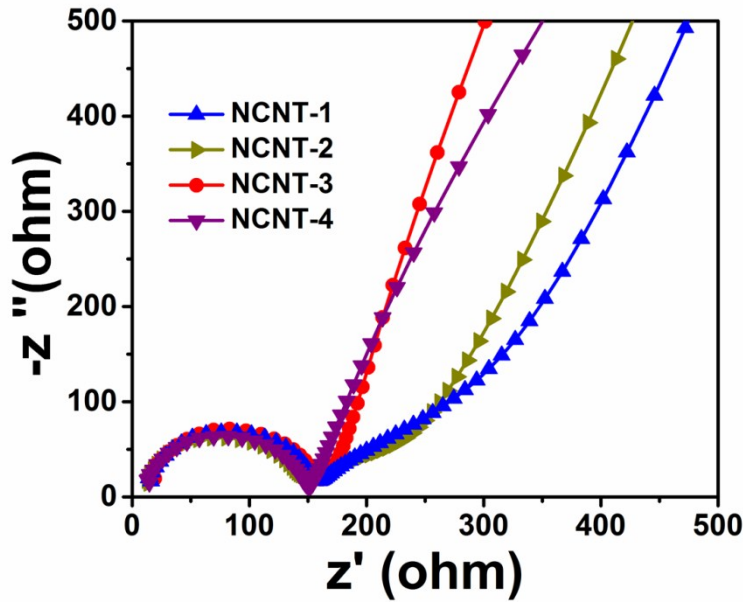


Fig. S11 EIS spectra of NCNT-x ($x = 1, 2, 3$ and 4 , respectively).

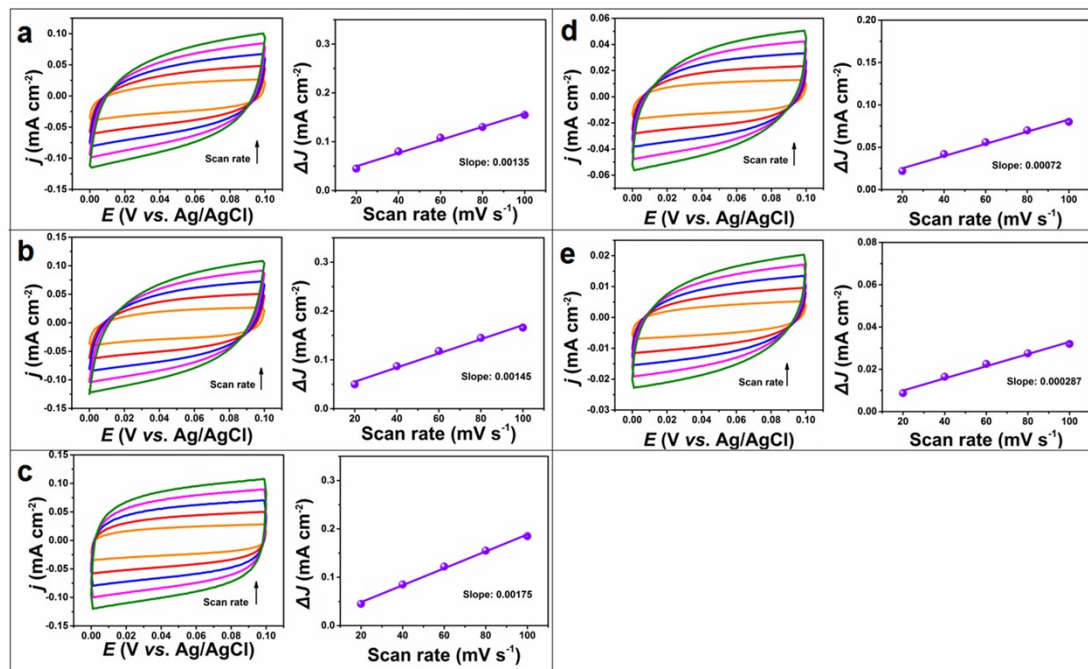


Fig. S12 CV curves at various scan rates ($20, 40, 60, 80$ and 100 mV/s) in the potential range $1\text{--}1.1$ V vs. RHE for NCNT-x ($x = 1, 2, 3$ and 4 , respectively) and CNT-P800 catalyst in 0.1 M KOH.

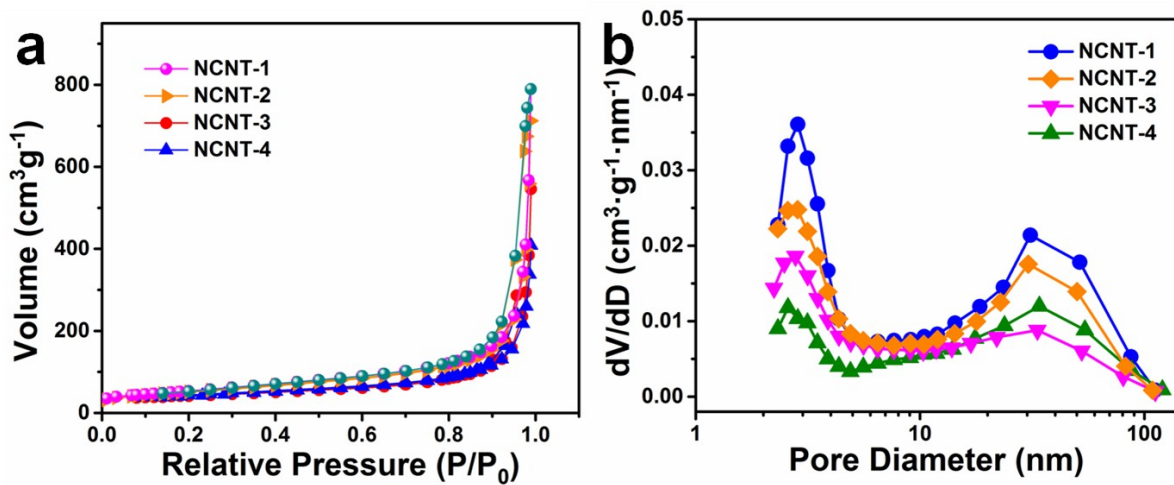


Fig. S13 (a) N₂ sorption isotherms and (b) the pore size distribution of NCNT-x (x= 1, 2, 3 and 4, respectively).

Table S9. The surface area of NCNT-x (x= 1, 2, 3 and 4, respectively)

Sample	BET surface area (m ² g ⁻¹)
NCNT-1	192.47
NCNT-2	181.91
NCNT-3	151.02
NCNT-4	149.46

Table S10. ORR performance of different catalysts (the electrolyte is 0.1 M KOH)

Catalyst	Loading (mg cm ⁻²)	E _{onset} vs. RHE (V)	E _{1/2} vs. RHE (V)	Current density (mA cm ⁻² at 0.4V)	Ref.
N-doped CNT arrays	Unknown	0.96	/	/	S1
N-doped CNTs	0.204	0.853	0.654	/	S2
EDA-NCNT	Unknown	0.94	0.81	4.91	S3

Winged N-doped CNTs	0.222	0.93	0.79	4.24	S4
N-CNT-1030	0.0813	0.91	0.694	4.80	S5
N-doped 3D GFs	0.012	0.78	/	1.20	S6
CNT@NCNT	0.025	0.94	/	/	S7
N-Carbon nanosheets	0.6	0.954	0.834	5.11	S8
CNTs@PPy-P800	0.2	0.95	0.81	6.72	This work

References

- S1 K. Gong, F. Du, Z. Xia, M. Durstock and L. M. Dai, *Science.*, 2009, **323**, 760.
- S2 Z. Chen, D. Higgins and Z. Chen, *Carbon.*, 2010, **48**, 3057.
- S3 Z. Chen, D. Higgins, H. Tao, R. S. Hsu and Z. Chen, *J. Phys. Chem. C.*, 2009, **113**, 21008.
- S4 Y. Cheng, H. Zhang, C. V. Varanasi and J. Liu, *Sci. Rep.*, 2013, **3**, 3195.
- S5 R. Du, N. Zhang, J. H. Zhu, Y. Wang, C. Y. Xu, Y. Hu, N. N. Mao, H. Xu, W. J. Duan, L. Zhuang, L. T. Qu, Y. L. Hou and J. Zhang, *Small.*, 2015, **11**, 3903.
- S6 Y. Zhao, C. Hu, Y. Hu, H. Cheng, G. Shi and L. Qu, *Angew. Chem.*, 2012, **124**, 11533.
- S7 G. L. Tian, Q. Zhang, B. Zhang, Y. G. Jin, J. Q. Huang, D. S. Su and F. Wei, *Adv. Funct. Mater.*, 2014, **24**, 5956.
- S8 W. Wei, H. Liang, K. Parvez, X. Zhuang, X. Feng and K. Müllen, *Angew. Chem. Int. Ed.*, 2014, **53**, 1596.